COMPARISON OF DIFFUSION MRI PREDICTIONS AND HISTOLOGY IN THE MACAQUE BRAIN

Stamatios N Sotiropoulos[1], Charlie Chen[2], Krikor Dikranian[2], Saad Jbabdi[1], Timothy EJ Behrens[1], David C Van Essen[2], and Matthew F Glasser[2]

[1]*FMRIB Centre, University of Oxford, Oxford, Oxfodshire, United Kingdom,* [2]*Department of Anatomy & Neurobiology, Washington University, St Louis, MO, United States*

Target Audience: This work will be of immediate interest to scientists studying low-level modelling for diffusion MRI and white matter tractography approaches, as well as scientists working on validation of diffusion MRI model predictions.

Purpose: Diffusion-weighted (DW) MRI uses the random thermal motions of water molecules to probe tissue micrustructure and fibre bundle orientation [1]. DW-MRI provides unique information about the living brain in terms of local structural features and long-range anatomical connectivity, but validation is challenging, given the paucity of ground truth data. Several studies have been recently conducted for developing validation frameworks for diffusion MRI [2-6]. Here we present a validation approach using myelin-stained histological sections of macaque cortex to map the neuronal fibre organisation. We use image processing approaches to extract ground truths on anatomical features of the underlying fibres, particulalry near the boundary between gray and white matter, where axonal trajectories are complex and not well characterised. We compare these features with predictions from model-based analysis of macaque DW-MRI scans. This includes predictions made for the major fibre orientation and for within-voxel fibre dispersion, a potentially important measure recently shown to be estimable from DW-MRI [7,8].

Methods: Histological preparation and diffusion MRI acquisition are described in detail in the following sections.

Histology: A postnatal day 6 macaque brain (Fig. 1) was perfusion-fixed with 4% paraformaldehyde, postfixed for 24 hrs (4° C) and sectioned coronally (70 μm) by Vibratome. Floating sections were immunostained with antibody to myelin basic protein (MBP, MAB395, Millipore) at 1:100 dilution and using Vactastain (Vector, USA) immunodetection kit with VIP (Vector) as chromogen. After mounting, dehydration and coverslipping, sections were scanned on a NanoZoomer 2 (Hamamatsu) scanning microscope equipped with Olympus lens at 20X (9.225 μm x 9.225 μm resolution). A modified Gallyas myelin stained section from an adult macaque was also digitized in a similar fashion (Fig. 2) [9].

Image Processing: Histological sections were processed using pixelwise structure tensor analysis [3,10]. Intensity gradients were calculated on grayscale images, after smoothing using a 2D Gaussian kernel (to increase stability in gradient calculation). A structure tensor was then obtained for each pixel, using the gradients of the pixel's local neighborhood. The eigenvector of the structure tensor corresponding to the smallest eigenvalue gave the *coherence* direction, i.e. the direction along which the image intensity exhibits the lowest fluctuations [11]. Fig. 1B presents these orientations using a red-green color-coding scheme (red:top-bottom and green: left-right). These pixelwise directions provide a good description of the underlying neuronal fibre orientations, as traced by the histological staining process.

Post-mortem DW-MRI: The data described in [7], [12] were utilised. In brief, a diffusion-weighted MRI dataset of a perfusion-fixed adult macaque brain was acquired using a 4.7 T Bruker scanner. Scans were performed using a 3D multi-shot, spin-echo sequence (acquisition matrix 128 × 142 with in-plane resolution 430 × 430 μm^2, TE = 33 ms, TR = 350 ms). Seventeen non-DW images were acquired, while diffusion weighting was applied along 120 uniformly distributed directions with b = 8000 s/mm^2. 128 slices were acquired with a thickness of 430 μm. Total imaging time was 27 h. The ball and stick model [13] and the ball and racket model [7] were fitted to the data to obtain estimates of the main fibre orientation and the within-voxel fibre dispersion, for each voxel.

Results & Discussion: We focused our analysis on the superior frontal gyrus of the left hemisphere (Fig. 1A). This was chosen due to the presence of unbroken radial fibers, indicating the section was cut near-orthogonal to the radial axis and could be compared to MRI sections of an equivalent region. After performing structure tensor analysis, the histological image was downsampled to match the MRI spatial resolution. The fibre (*coherence*) orientations (Fig. 1B) were regrouped (Fig. 1C), to provide a measure of within-plane fibre orientation dispersion at the MRI resolution. This ground-truth was compared to the dispersion predictions made from DW-MRI, using the ball and racket model (Fig. 1D). Despite the 2D (histology) vs 3D (MRI) nature of the two dispersion maps, they agree qualitatively in many aspects. Both exhibit increased dispersion, as fibres fan out to the cortex (blue circle) or exhibit incoherence due to bending/fanning in deeper white matter (yellow circle). Furthermore, they both predict reduced dispersion near the fundus of a sulcus (white arrow).

We further compared the main fibre orientations, as revealed by histology and DW-MRI using the ball & stick model [13]. A path defining the gray-white matter boundary was manually delineated (Fig. 2 left). Points were selected along the boundary at intervals of 0.43mm to approximate the dimensions of an MRI voxel (point 0 at the gyral crown). At each point, the angle of the main fibre orientation (from histology and as predicted by DW-MRI) with the normal to the boundary was obtained at three positions (Fig. 2 left): a) before the boundary, within white matter (red), b) at the boundary (blue) and c) after the boundary, entering the cortex (green). These angles were plotted as a function of the distance from the gyral crown for each of the three positions (red, blue and green respectively). As shown in Fig. 2 (right), there is good agreement between the angles predicted from histology (solid lines) and those predicted by diffusion MRI (dashed lines). A substantial discrepancy is observed only along limited regions of the gray-white matter boundary (blue orientations, voxels 8-12), where the fibre orientations change acutely before and after the boundary.

These results were obtained by comparing (2D) histology and (3D) MRI scans of different subjects. Therefore, despite their qualitative nature, they are very encouraging for the model-based DW-MRI predictions. We are working towards more quantitative comparative frameworks that will improve limitations of the current work (for instance, perform histology and MRI on the same subject; use more regions for validation).

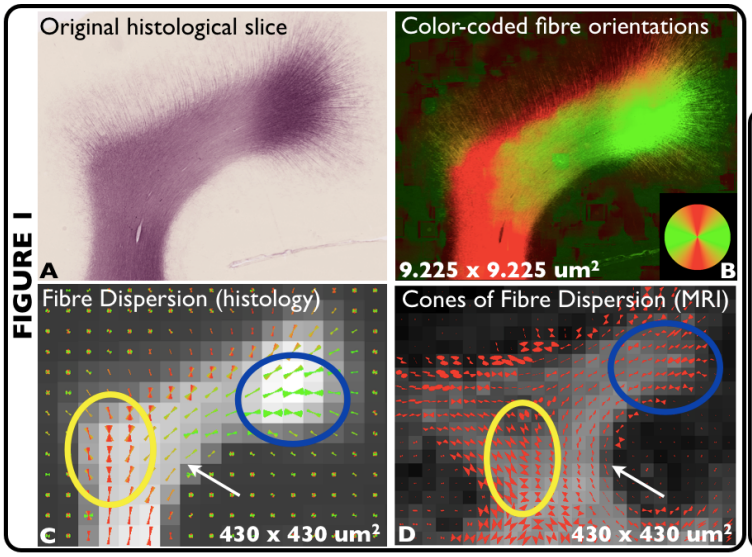

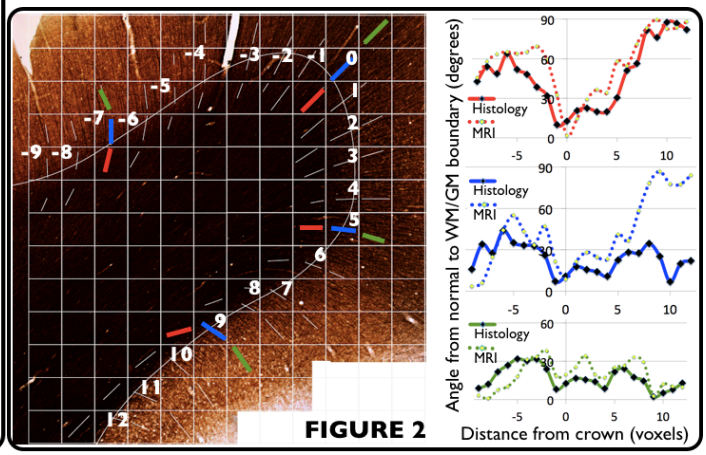

References: **[1]** Beaulieau, NMR Biomed 15:435-55, 2002. **[2]** Calamante et al, Neuroimage 59:286-296, 2012. **[3]** Budde et al, Neuroimage 63, doi:10.1016/j.neuroimage.2012.06.042, 2012. **[4]** Takahashi et al, Cereb Cortex 21:200-211, 2011. **[5]** Hansen et al, Neuroimage 57:1458-1465, 2011. **[6]** Jespersen et al, IEEE TMI 31:16-32, 2012. **[7]** Sotiropoulos et al, Neuroimage 60:1412-1425, 2012. **[8]** Zhang et al, Neuroimage 61:1000-1016, 2012. **[9]** Carmichael et al, J Comp Neurol 346: 366-402, 1994. **[10]** Bigun & Granlund, IEEE ICCV:433-438, 1987. **[11]** Weickert, Int J Comp Vis 31:111-127, 1999. **[12]** D'Arceuil et al, Neuroimage 35:553-565, 2007. **[13]** Behrens et al, Neuroimage 34:144-155, 2007.

Acknowledgement: We ackowledge support from the Human Connectome Project (1U54MH091657-01), NIMH R01-MH-60974, the Hope Center Alafi Neuroimaging Lab, and a P30 Neuroscience Blueprint Interdisciplinary Center Core award to Washington University (P30 NS057105).